and combustion of conventional hydrocarbons. In such cases the increase in pressure drag due to blowing is largely offset by the reduction in friction drag and hence the weak dependence of C_D on mass transfer. However, in the presence of excessive volatility, friction drag essentially vanishes, resulting in the deterioration of the Renksizbulut-Yuen correlation.

References

[1]Lee, A., Law, C. K., and Randolph, A. L., "Aerothermochemical Studies of Energetic Liquid Materials. 2. Combustion and Microexplosion of Droplets of Organic Azides," *Combustion and Flame,* Vol. 71, No. 2, 1988, pp. 123–136.

[2]Haywood, R. J., Nafziger, R., and Renksizbulut, M., "A Detailed Examination of Gas and Liquid Phase Transient Processes in Convective Droplet Evaporation," *Journal of Heat Transfer,* Vol. 111, No. 2, 1989, pp. 495–502.

[3]Renksizbulut, M., and Haywood, R. J., "Transient Droplet Evaporation with Variable Properties and Internal Circulation at Intermediate Reynolds Numbers," *International Journal of Multiphase Flow,* Vol. 14, No. 2, 1988, pp. 189–202.

[4]Renksizbulut, M., and Yuen, M. C., "Experimental Study of Droplet Evaporation in a High-Temperature Air Stream," *Journal of Heat Transfer,* Vol. 105, No. 2, 1983, pp. 384–388.

[5]Renksizbulut, M., and Yuen, M. C., "Numerical Study of Droplet Evaporation in a High-Temperature Air Stream," *Journal of Heat Transfer,* Vol. 105, No. 2, 1983, pp. 389–397.

[6]Cliffe, K. A., and Lever, D. A., "Isothermal Flow Past a Blowing Sphere," Theoretical Physics Division, Atomic Energy Research Establishment, Harwell, Oxfordshire, England, UK, TP.1042, May 1984.

Dusty Supersonic Viscous Flow over a Two-Dimensional Blunt Body

R. Elangovan* and H. V. Cao†

Boeing Airplanes, Wichita, Kansas

Nomenclature

c = sound speed, $\bar{c}/\bar{u}_\infty$
C_D = drag coefficient of particle
$\bar{C}_p$ = gas specific heat at constant pressure, J/kg-K
$\bar{C}_v$ = gas specific heat at constant volume, J/kg-K
$\bar{C}_m$ = specific heat of particle material, J/kg-K
$\bar{L}$ = reference length, m
M_∞ = freestream Mach number
p = pressure, $\bar{p}/\bar{\rho}_\infty \bar{u}_\infty^2$
Pr = Prandtl number
$\bar{R}$ = gas constant, J/kg-K, or leading-edge radius, m
Re_L = Reynolds number based on characteristic length, $\bar{\rho}_\infty \bar{u}_\infty \bar{L}/\bar{\mu}_\infty$
Re_p = Reynolds number based on particle diameter [see Eq. (5)]
Re_r = relative Reynolds number [see Eq. (4)]
T = gas temperature, $\bar{T}/\bar{T}_\infty$
T_p = particle temperature, $\bar{T}_p/\bar{T}_\infty$
$\bar{T}_\infty$ = freestream gas temperature, K
u = gas velocity component in x direction, $\bar{u}_p/\bar{u}_\infty$
u_p = particle velocity component in x direction, $\bar{u}_p/\bar{u}_\infty$
$\bar{u}_\infty$ = freestream gas velocity, m/s
v = gas velocity component in y direction, $\bar{v}/\bar{u}_\infty$
v_p = particle velocity component in y direction, $\bar{v}_p/\bar{u}_\infty$
x,y = Cartesian coordinates in physical space, $x = \bar{x}/\bar{L}$, $y = \bar{y}/\bar{L}$
Γ = particle material specific heat ratio, $\bar{C}_m/\bar{C}_p$
γ = gas specific heat ratio, $\bar{C}_p/\bar{C}_v$
δ = freestream loading ratio, $\bar{\rho}_{p\infty}/\bar{\rho}_\infty$
μ = gas viscosity, $\bar{\mu}/\bar{\mu}_\infty$
$\bar{\mu}_\infty$ = freestream gas viscosity, kg/s-m
ρ = gas phase density, $\bar{\rho}/\bar{\rho}_\infty$
$\bar{\rho}_m$ = density of particle material, kg/m^3
ρ_p = particle phase density, $\bar{\rho}_p/\bar{\rho}_\infty$
$\bar{\rho}_\infty$ = freestream gas density, kg/m^3
$\bar{\sigma}$ = particle radius, μm
τ_T = temperature relaxation time [see Eq. (3)]
τ_v = velocity relaxation time [see Eq. (2)]
$(\bar{\ })$ = dimensional quantities

I. Introduction

DUSTY gas flows have been studied by a number of authors[1-8] in the past due to applications of the flows in rocket nozzle flow, supersonic flight through dust clouds, in the prediction of erosion damage caused by dust particles, and in flow-measuring instruments that use particles as tracers. In such two-phase flows, the gas phase and particle phase may have different velocities and temperatures, and as a consequence the two phases interact through viscous drag and heat transfer. As a result of the interaction, the gas phase flowfield differs from its corresponding pure gas flowfield. When a two-phase flow encounters a disturbance such as a shock wave, nonequilibrium is created between the two phases, and some relaxation distance is required before the gas and particle phases obtain a new equilibrium state.

Numerous inviscid analytical and numerical solutions of dusty supersonic flow over simple two-dimensional geometries, such as wedges and cones with attached shocks, can be found in the literature.[2,5-7] All of these solutions are based on the method originally proposed by Carrier.[9] The Carrier method anlysis requires the specification of gas and particle properties behind the gasdynamic shock as initial conditions for numerical integration. The determination of gas properties behind the gasdynamic shock requires knowledge of the shock location and shape. In a recent investigation,[10] which is also based on the Carrier method, inviscid dusty supersonic flow over a blunt axisymmetric body with a detached shock was treated. The solution technique used in the investigation is the so-called inverse method in which the shock shape is specified and the flowfield and body shape are numerically determined.

In problems of practical interest, neither the shock position nor the shape is known beforehand. When a detached bow shock wave is present, the gas properties behind the shock required for numerical solution cannot be determined accurately. The presence of multiple shocks complicates the problem further, since both the gas and the particle properties needed for numerical solution are not known due to the equilibration process taking place between the shocks. In this paper, a general direct numerical method for solving the full dusty gas viscous flow equations is presented. The numerical method is validated by comparing the normal shock structure solution obtained by solving the two-dimensional equations using the present method with that of the Carrier method solution. The present method is also used to compute the dusty gas flowfield over a two-dimensional blunt body.

II. Model Equations

The basic equations of motion governing dusty viscous flow[1] in two dimensions can be written in conservation form as

$$\frac{\partial U}{\partial t} + \frac{\partial F}{\partial x} + \frac{\partial G}{\partial y} = H \tag{1}$$

Presented as Paper 89-0686 at the AIAA 27th Aerospace Sciences Meeting, Reno, NV, Jan. 9–12, 1989; received Feb. 9, 1989; revision received Jan. 2, 1990.

*Senior Specialist Engineer, Concept Development Group. Member AIAA.

†Specialist Engineer, Computational Fluid Dynamics Staff; currently, Aerodynamics Research, Boeing Commercial Airplane Group, Seattle, WA. Member AIAA.

where

$$U = \begin{bmatrix} \rho \\ \rho u \\ \rho v \\ E \\ \rho_p \\ \rho_p u_p \\ \rho_p v_p \\ E_p \end{bmatrix}; \quad F = \begin{bmatrix} \rho u \\ \rho u^2 + p - \tau_{xx} \\ \rho u v - \tau_{xy} \\ u(E+p) - u\tau_{xx} - v\tau_{xy} + q_x \\ \rho_p u_p \\ \rho_p u_p^2 \\ \rho_p u_p v_p \\ u_p E_p \end{bmatrix}$$

$$G = \begin{bmatrix} \rho v \\ \rho u v - \tau_{xy} \\ \rho v^2 + p - \tau_{yy} \\ v(E+p) - u\tau_{xy} - v\tau_{yy} + q_y \\ \rho_p v_p \\ \rho_p u_p v_p \\ \rho_p v_p^2 \\ v_p E_p \end{bmatrix}$$

$$H = \begin{bmatrix} 0 \\ F_{px} \\ F_{py} \\ Q_p + u_p F_{px} + v_p F_{py} \\ 0 \\ -F_{px} \\ -F_{py} \\ -Q_p - u_p F_{px} - v_p F_{py} \end{bmatrix}$$

and where τ_{xx}, τ_{xy}, and τ_{yy} are the components of the shear-stress tensor, and q_x and q_y are the components of the heat-flux vector. The gas phase and particle phase total energy terms are given by

$$E = \frac{p}{\gamma - 1} + \frac{\rho}{2}(u^2 + v^2)$$

$$E_p = \frac{\Gamma \rho_p T_p}{(\gamma - 1)M_\infty^2} + \frac{\rho_p}{2}(u_p^2 + v_p^2)$$

If the drag coefficient for the particles is assumed to be of the form[11]

$$C_D = \frac{24}{Re_r}\left(1 + \frac{Re_r^{2/3}}{6}\right)$$

then, the drag force terms in nondimensional form are given by

$$F_{px} = \frac{\mu \rho_p}{\tau_v}\left(1 + \frac{Re_r^{2/3}}{6}\right)(u_p - u)$$

$$F_{py} = \frac{\mu \rho_p}{\tau_v}\left(1 + \frac{Re_r^{2/3}}{6}\right)(v_p - v)$$

$$\tau_v = \frac{4\bar{\rho}_m \bar{\sigma}^2 \bar{u}_\infty}{18 \bar{\mu}_\infty \bar{L}} \tag{2}$$

The heat transfer between the gas and particles is given by

$$Q_p = \frac{\Gamma \rho_p \mu}{(\gamma - 1)M_\infty^2 \tau_T} Nu(T_p - T)$$

$$\tau_T = \frac{4\Gamma Pr\, \bar{\rho}_m \bar{\sigma}^2 \bar{u}_\infty}{6 \bar{\mu}_\infty \bar{L}} \tag{3}$$

where the Nusselt number correlation used is of the following form[12]

$$Nu = 2 + 0.6 Pr^{1/3} Re_r^{1/2}$$

$$Re_r = Re_p\left(\frac{\rho}{\mu}\right)\left[(u_p - u)^2 + (v_p - v)^2\right]^{1/2} \tag{4}$$

$$Re_p = \frac{\bar{\rho}_\infty 2\bar{\sigma}\bar{u}_\infty}{\bar{\mu}_\infty} \tag{5}$$

In the formulation of the model equations, the main assumptions made are 1) the particles are assumed to be spherical in shape; 2) the number density of particles is sufficiently large so that the particle cloud can be described by a set of continuum variables; 3) the volume fraction of the particles is small so that the collisions between individual particles can be neglected; and 4) the gas phase and particle phase interact exclusively through the drag force and the heat exchange between them.

III. Numerical Algorithm

The explicit predictor-corrector equations for approximating Eq. (1) are

Predictor:

$$\overline{U_{i,j}^{n+1}} = U_{i,j}^n - \Delta t\left[\frac{F_{i+1,j}^n - F_{i,j}^n}{\Delta x} + \frac{G_{i,j+1}^n - G_{i,j}^n}{\Delta y} - H_{i,j}^n\right] \tag{6}$$

Corrector:

$$U_{i,j}^{n+1} = \frac{1}{2}\left[U_{i,j}^n + \overline{U_{i,j}^{n+1}} - \Delta t\left(\frac{\overline{F_{i+1,j}^{n+1}} - \overline{F_{i,j}^{n+1}}}{\Delta x} + \frac{\overline{G_{i,j+1}^{n+1}} - \overline{G_{i,j}^{n+1}}}{\Delta y} - \overline{H_{i,j}^{n+1}}\right)\right] \tag{7}$$

where

$$H_{i,j}^m = \frac{1}{\Delta x \Delta y}\int_{y_j - \Delta y/2}^{y_j + \Delta y/2}\int_{x_i - \Delta x/2}^{x_i + \Delta x/2} H^m \,\mathrm{d}x\,\mathrm{d}y$$

$$m = n \text{ or } \overline{n+1}$$

The double integral over H is evaluated numerically over a grid cell spacing using trapezoidal rule quadrature. The first step [Eq. (6)] predicts a new solution at time $t = (n+1)\Delta t$ at each mesh point i,j from the known solution at time $t = n\Delta t$ and uses a one-sided difference to approximate the first derivative and a centered difference for the second derivative. The second step [Eq. (7)] corrects the predicted values with an opposite one-sided difference for the first derivative. This differencing procedure is similar to the MacCormack explicit method[13] and is second-order accurate. Since the particle relaxation time scales are larger than the fluid dynamic time scale, the maximum computational time step is given by the CFL and viscous stability requirement for the MacCormack method.

IV. Normal Shock and Relaxation Zone Structure

The normal shock and relaxation zone structure proposed by Carrier[9] consists of 1) an equilibrium mixture ahead of the shock (state 1), 2) a gasdynamic shock $1 \rightarrow 2$, where, as a result of the transition through the shock front, a nonequilibrium condition is suddenly established, 3) a relatively thick nonequilibrium zone in which the velocity- and temperature-equilibration processes take place $2 \rightarrow 3$, and 4) a new equilibrium of the particle with the gas (state 3). The rationale for the separation of these zones is that the volume fraction of particles is negligible and the gasdynamic shock structure is unaffected by the particle cloud. Since the time in which a particle crosses the shock front is about two to three orders of magnitude smaller than both the velocity- and temperature-relaxation time, the particle crosses the shock front with negligible change in velocity and temperature. Thus, the properties of the particle immediately behind the shock front (state 2) are the same as the properties at the equilibrium state upstream of the shock front (state 1).

$$u_{p2} = u_{p1}, \qquad T_{p2} = T_{p1} \tag{8}$$

The properties of the gas at state 2 are given by the Rankine-Hugoniot relations. For steady one-dimensional flow, choosing state 1 conditions as reference conditions (∞), the models of Eq. (1) can be expressed in the following form.

A. Gas Phase

The continuity equation becomes

$$\rho u = \rho_3 u_3 = 1$$

Using the particle phase equations, the gas phase momentum and energy equations can be written as

$$\frac{du}{dx} = \frac{3Re_L}{4}\left(\frac{1}{\mu}\right)\left[\frac{1}{\gamma M_\infty^2}\frac{T}{u} + u + \delta u_p - A\right] \tag{9}$$

Using the particle phase energy and continuity equations, the gas phase energy equation can be written as

$$\frac{dT}{dx} = (\gamma+1)M_\infty^2 Pr Re_L\left(\frac{1}{\mu}\right) \times \left[\frac{1}{\gamma(\gamma-1)M_\infty^2}T - \frac{u^2}{2} + Au - \delta u u_p + \frac{\delta}{2}u_p^2 + \frac{\delta\Gamma}{(\gamma-1)M_\infty^2}T_p - B\right] \tag{10}$$

where

$$A = 1 + \delta + \frac{1}{\gamma M_\infty^2}; \qquad B = \frac{1+\delta}{2} + \frac{1+\delta\Gamma}{(\gamma-1)M_\infty^2}$$

B. Particle Phase

The particle phase continuity, momentum, and energy equations become

$$\rho_p u_p = \rho_{p3} u_{p3} = \delta$$

$$\frac{du_p}{dx} = -\frac{\mu}{\tau_v}\left(1 + \frac{Re_r^{2/3}}{6}\right)\frac{u_p - u}{u_p} \tag{11}$$

$$\frac{dT_p}{dx} = -\frac{\mu}{\tau_T}\left(2 + 0.6 Pr^{1/3} Re_r^{1/2}\right)\frac{T_p - T}{u_p} \tag{12}$$

where

$$Re_r = Re_p(\rho/\mu)|u_p - u|$$

Given the initial conditions at state 2, the four coupled ordinary differential equations (9–12) can be integrated for the gas phase and particle phase velocity and temperature. The initial conditions for the particle phase are the frozen conditions given by Eq. (8). For the gas phase, the initial conditions are the Rankine-Hugoniot relations.

To compute the normal shock and relaxation zone structure using the finite-difference algorithm, the pressure at the equilibrium condition (state 3) must be specified. The equilibrium pressure p_3 can be expressed in terms of state 1 quantities as follows. The shock relations for the dusty gas flow are

$$\rho_3 u_3 = \rho_1 u_1$$

$$\rho_{p3} u_{p3} = \rho_{p1} u_{p1} = \delta$$

$$p_3 + \rho_3 u_3^2 + \rho_{p3} u_{p3}^2 = p_1 + \rho_1 u_1^2 + \rho_{p1} u_{p1}^2$$

$$u_3(E_3 + p_3) + u_{p3}E_{p3} = u_1(E_1 + p_1) + u_{p1}E_{p1}$$

Equation of state:

$$p_i = \frac{\rho_i T_i}{\gamma M_\infty^2}$$

Equilibrium conditions:

$$u_{p1} = u_1, \qquad T_{p1} = T_1$$

$$u_{p3} = u_3, \qquad T_{p3} = T_3$$

Choosing the state 1 conditions as reference conditions (∞), the shock relations are solved for the equilibrium pressure p_3 and given by

$$p_3 = \frac{2\hat{\gamma}\hat{M}_\infty^2 - (\hat{\gamma}-1)}{\gamma M_\infty^2(\hat{\gamma}+1)} \tag{13}$$

where

$$\hat{\gamma} = \frac{\gamma(1+\delta\Gamma)}{1+\delta\gamma\Gamma}; \qquad \hat{M}_\infty^2 = \frac{(1+\delta)(1+\delta\gamma\Gamma)}{1+\delta\Gamma}M_\infty^2$$

The normal shock and relaxation zone structure was computed employing the present finite-difference algorithm, Eqs. (6) and (7). The problem was treated in two dimensions with a 101×6 plane mesh. The particles selected were uniform size glass spheres of radius $\bar{\sigma} = 2\ \mu$m. The particle properties used and the loading ratio specified were

$$\bar{C}_m = 835 \text{ J/kg-K}, \qquad \bar{\rho}_m = 2225 \text{ kg/m}^3, \qquad \delta = 0.5$$

For air the properties used were

$$\bar{R} = 287.074 \text{ J/kg-K}, \qquad \bar{C}_p = 1007 \text{ J/kg-K}$$

$$\gamma = 1.4, \qquad Pr = 0.72$$

The freestream conditions specified were

$$M_\infty = 6, \qquad \bar{T}_\infty = 300 \text{ K}$$

$$Re_L = 1.3278 \times 10^4, \qquad \bar{L} = 1 \times 10^{-4} \text{ m}$$

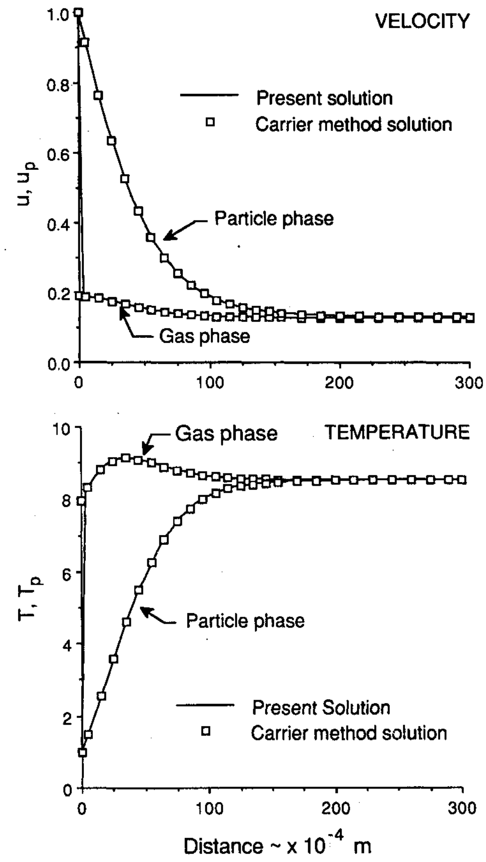

Fig. 1 Normal shock and relaxation zone structure (Mach = 6). Comparison of present finite difference and Carrier method solutions.

The upstream boundary conditions are the freestream conditions, where the gas and particle phases are in equilibrium. The particle phase density is the specified particle loading. The downstream boundary condition specified is the equilibrium gas pressure p_3 given by Eq. (13). The present finite-difference solution and the Carrier method solution are shown in Fig. 1 and are identical in the relaxation zone. The present method also resolves the gasdynamic shock profile accurately.

V. Two-Dimensional Blunt Body

The geometry selected for the dusty gas calculation was a 20 deg wedge having a 1 cm radius circular arc blunt leading edge. The model equations were transformed to general curvilinear coordinates and expressed in conservation-law form. A 121×49 C-mesh with clustering near the body surface for viscous flow calculation was generated using GRAPE.[14] After an initial flow calculation, the shock region was identified and the mesh was refined in that region using the Eiseman control function.[15]

Far-field boundary conditions imposed were all flow variables specified at the supersonic inflow boundary and extrapolated at the supersonic outflow boundary. At the solid wall surface, no slip and an adiabatic temperature boundary condition were used for the gas phase. For the particle phase, it was assumed in the present investigation that the particles either stick to the body or break after colliding with the body to form much smaller particles, which then form a thin dusty layer at the body surface.[10] Hence, an adiabatic particle phase temperature boundary condition was used, and the remaining particle phase flow variables were extrapolated from the grid points just above the solid surface.

The pure gas calculation was made first. The freestream conditions specified were

$$M_\infty = 3, \qquad \delta = 0, \qquad \bar{T}_\infty = 300 \text{ K}$$
$$Re_L = 1.2 \times 10^5, \qquad \bar{R} = 0.01 \text{ m}$$

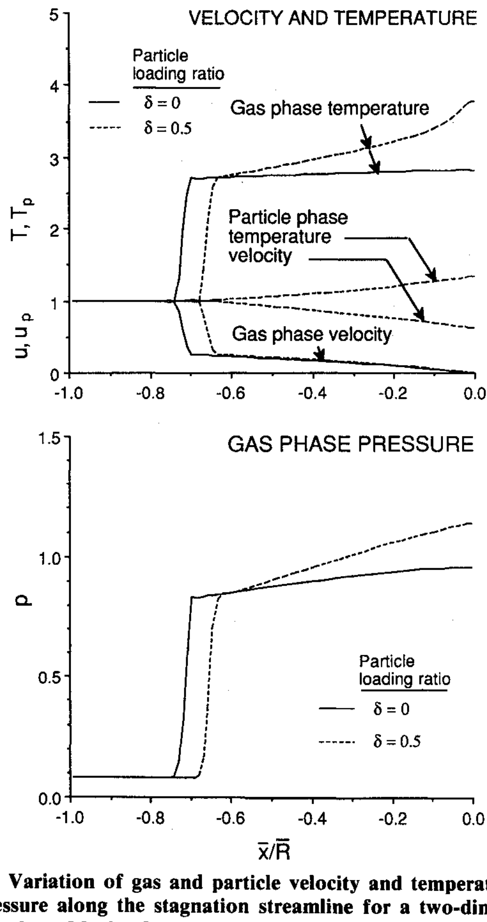

Fig. 2 Variation of gas and particle velocity and temperature, and gas pressure along the stagnation streamline for a two-dimensional blunt body at Mach = 3.

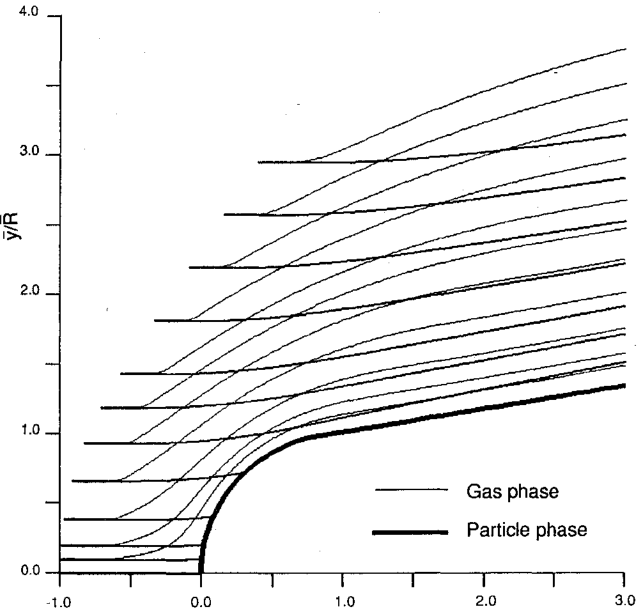

Fig. 3 Gas and particle streamlines around a two-dimensional blunt body at Mach = 3.

Next, for the same freestream conditions and for $\bar{\sigma} = 2$ μm, $\delta = 0.5$, the dusty gas calculation was made. Figure 2 shows the computed pure gas ($\delta = 0$) and dusty gas ($\delta = 0.5$) velocity, temperature, and pressure along the stagnation streamline. The gas and particle streamlines around the blunt body are shown in Fig. 3.

In the pure gas case, the present computed shock standoff distance is 0.71 cm and agrees well with the inviscid calculation standoff distance values presented in Ref. 16. The computed stagnation pressure and temperature values are $p = 0.953$ and $T = 2.823$, and the exact isentropic values are $p = 0.957$ and $T = 2.83$, respectively. In the dusty gas case, the computed shock standoff distance is 0.65 cm. The gas phase stagnation pressure and temperature values are $p = 1.134$, and $T = 3.774$, and the particle temperature value is $T_p = 1.345$. As can be seen, the particle temperature T_p does not reach the gas temperature T. Near the stagnation region, the particle velocity u_p does not reach the gas velocity u, and a slip velocity $(u_p - u)$ always exists. Hence, heat is generated in the gas phase due to the work done by the particles passing through the gas. In the case of particle phase, the temperature T_p does not increase very much, that is, the heat transferred from the gas to the particle is slight.

Acknowledgments

The authors would like to thank C. M. Hung of the NASA Ames Research Center for many valuable discussions and the reviewers for their suggestions.

References

[1]Marble, F. E., "Dynamics of Dusty Gases," *Annual Review of Fluid Mechanics,* Vol. 2, 1970, pp. 397–446.

[2]Rudinger, G., *Fundamentals of Gas-Particle Flows,* Elsevier, Amsterdam, 1980.

[3]Soo, S. L., *Fluid Dynamics of Multiphase Flows,* Blaisdell, Waltham, MA, 1967.

[4]Gilbert, M., Allport, J., and Dunlap, R., "Dynamics of Two-Phase Flow in Rocket Nozzles," *ARS Journal,* Vol. 32, 1962, pp. 1929–1930.

[5]Probstein, R. F., and Fassio, F., "Dusty Hypersonic Flows," *AIAA Journal,* Vol. 8, 1970, pp. 772–779.

[6]Waldman, G. D., and Reinecke, W. G., "Particle Trajectories, Heating, and Breakup in Hypersonic Shock Layers," *AIAA Journal,* Vol. 9, 1971, pp. 1040–1048.

[7]Peddieson, J., "Gas-Particle Flow Past Bodies with Attached

Shock Waves," *AIAA Journal,* Vol. 13, 1975, pp. 939–941.
[8]Moon, L. F., "High Power Laser Mixing and Reacting Flow Characterization," Sec. D1, Bell Aerospace Co., Rept. No. 9500-920309, 1973.
[9]Carrier, G. F., "Shock Waves in a Dusty Gas," *Journal of Fluid Mechanics,* Vol. 4, 1958, pp. 376–382.
[10]Sugiyama, H., "Numerical Analysis of Dusty Supersonic Flow Past Blunt Axisymmetric Bodies," Univ. of Toronto Inst. for Aerospace Studies, Rept. No. 267, 1983.
[11]Putnam, A., "Integrable Form of Droplet Drag Coefficient," *ARS Journal,* Vol. 31, 1961, pp. 1467–1468.
[12]Knudsen, J. G., and Katz, D. L., *Fluid Dynamics and Heat Transfer,* McGraw-Hill, New York, 1958.
[13]MacCormack, R. W., "The Effect of Viscosity in Hypervelocity Impact Cratering," AIAA Paper 69-354, 1969.
[14]Sorenson, R., "A Computer Program to Generate Two-Dimensional Grids About Airfoils and Other Shapes by the Use of Poisson's Equation," NASA TM-81198.
[15]Eiseman, P., "Grid Generation for Fluid Mechanics Computations," *Annual Review of Fluid Mechanics,* Vol. 17, 1985, pp. 487–522.
[16]Hamilton, H. H., "Solution of Axisymmetric and Two-Dimensional Inviscid Flow Over Blunt Bodies by the Method of Lines," NASA TP-1154, 1978.

Natural Convection from Isothermal Plates Embedded in Thermally Stratified Porous Media

F. C. Lai*
Colorado State University,
Fort Collins, Colorado 80523
I. Pop†
University of Cluj, Cluj, Romania
and
F. A. Kulacki‡
Colorado State University,
Fort Collins, Colorado 80523

Nomenclature

A = constant, Eq. (4)
f = dimensionless stream function, Eq. (6)
G = auxiliary function, Eq. (14)
g = acceleration due to gravity
h = local heat-transfer coefficient
K = permeability of porous medium
k = effective thermal conductivity of porous medium
Nu = local Nusselt number, hx/k
q = local heat flux
Ra = local Rayleigh number, $Kg\beta(T_w - T_{\infty,o})x/\alpha\nu$
T = temperature
ΔT = temperature difference between the wall and porous medium, $T_w - T_\infty$
u,v = x and y velocity components
x,y = vertical and horizontal coordinates
α = thermal diffusivity
β = coefficient of thermal expansion
ϵ = dimensionless vertical distance, $Ax^\lambda/(T_w - T_{\infty,o})$
η = dimensionless horizontal distance, Eq. (5)
θ = dimensionless temperature, Eq. (7)
λ = constant, Eq. (4)
ν = kinematic viscosity
ξ = nonsimilarity variable
ϕ = auxiliary function, Eq. (14)
ψ = stream function

Subscripts

iso = quantity related to the uniform porous medium
o = leading edge of the plate
w = wall
∞ = ambient

Received April 19, 1989; revision received Aug. 22, 1989.

*Research Associate, Department of Mechanical Engineering. AIAA Member.
†Professor, Department of Mathematics.
‡Professor and Dean, College of Engineering.

Introduction

NATURAL convection in porous media has recently received considerable attention for its important applications in many engineering problems. However, most previous studies have considered only a uniform environment. A thermally stratified field, although encountered frequently in many applications, has received rather little attention.

The first attempt to study natural convection in a thermally stratified porous medium was made by Johnson and Cheng.[1] Based on a general approach, they reached the conclusion that a similarity solution is not possible for the case of a stable stratification. Later, El-Khatib and Prasad[2] presented a numerical study on the effects of thermal stratification on natural convection in a horizontal porous layer with localized heating from below. Their results showed that the overall Nusselt number decreases with an increase in the thermal stratification. Recently, Nakayama and Koyama[3] extended the Johnson and Cheng study to report similarity solutions for that special case in which the ambient temperature increases inversely with the distance (i.e., $\Delta T \propto x^\lambda$, $\lambda<0$). It is felt, however, that such similarity solutions have limited application in practice due to the assumed temperature profile.

It is the purpose of this Note to extend previous studies by considering a more realistic temperature distribution which may be actually encountered in applications, e.g., ambient temperature varying with the distance ($\Delta T \propto x^\lambda$, $\lambda>0$). Since it has been pointed out by Johnson and Cheng[1] that similarity solutions are not possible for this case, series solutions and local nonsimilarity solutions are sought instead. It is expected that the solutions thus obtained will have useful applications in practice and will serve as a complement to the existing solutions.

Analysis

Consider a vertical plate embedded in an infinite porous medium (Fig. 1): The wall temperature is uniform at T_w, and the ambient temperature varies with distance from the leading

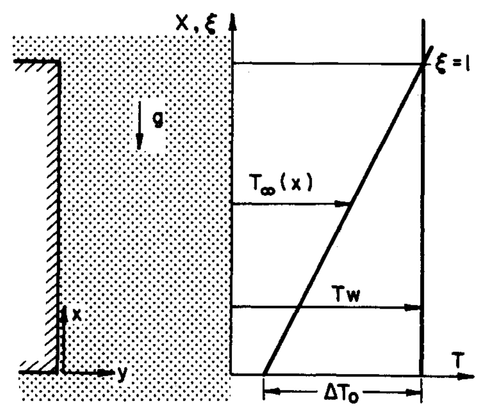

Fig. 1 Vertical plate in a thermally stratified porous medium.